A novel method for preparing BiOI nanoplates and its use as precursor to synthesize porous $BiVO_4$ water oxidation photocatalyst

Hoang V. Le,[a] Duc N. Nguyen,[b] Quyen T. Nguyen,[b] Ly T. Le,[b] Phong D. Tran[b*]

[a] *Institute of Science and Technology, TNU-University of Sciences, Thai Nguyen, Viet Nam.*

[b] *University of Science and Technology of Hanoi, Vietnam Academy of Science and Technology, 18 Hoang Quoc Viet, Hanoi, 100000 Vietnam.*

Email: tran-dinh.phong@usth.edu.vn

Supplementary

1. Synthesis of BiOI nanoplates: Optimization of KI: $Bi(NO_3)_3$ molar ratio

In order to optimize the composition of precursor solution, namely the KI: $Bi(NO_3)_3$ molar ratio, a fix molar concentration of $Bi(NO_3)_3$ of 0.04M was used while different KI concentration of 0.08, 0.16, 0.20, 0.24, 0.32, 0.40, 0.45, 0.48, and 0.60 M KI was assayed. For samples with KI concentration of 0.08, 0.16, 0.20, 0.24, and 0.32 M KI, namely the KI:$Bi(NO_3)_3$ molar ratio of smaller than 10:1, heterogeneous precursor mixture was generated (**Figure S10**). Whereas, with KI concentration of 0.40, 0.45, 0.48, and 0.60 M, namely the KI:$Bi(NO_3)_3$ molar ratio being equal or higher than 10:1, the homogeneous $[BiI_4]^-$ complex solution was generated from that BiOI nanoplate powder was obtained via the slow diffusion of NH_3 vapor. **Figures S11 and S12** show SEM images, XRD patterns and Raman spectra collected on these BiOI powders using different KI:$Bi(NO_3)_3$ molar ratio (of higher than 10:1).

2. Attempt preparation of BiOCl and BiOBr

Bismuth nitrate pentahydrate ($Bi(NO_3)_3.5H_2O$) and KCl (or KBr) were used as the Bi and Cl (or Br) source. For the preparation of BiOCl, 0.388 g $Bi(NO_3)_3.5H_2O$ was added into 20 mL of 0.45M KCl aqueous solution, immediately generating precipitates. The mixture was then further sonicated for 1 hour. After completion of the reaction, the precipitates were collected by centrifugation, washed three times with DI water, ethanol and finally dried in vacuum oven overnight. The BiOBr powder was synthesized using the same process.

The morphology and structure of resultant BiOCl and BiOBr powders were examined by SEM and XRD, as shown in **Figure S13** and **Figure S14**. **Figure S13** show that both BiOCl and BiOBr are aggregated nanoplates. **Figure S14** show the XRD patterns of BiOBr and BiOCl. All of the diffraction peaks can be clearly indexed as the tetragonal phase of BiOBr and BiOCl (JCPDS card 01-073-2061 and 01-085-0861, respectively).

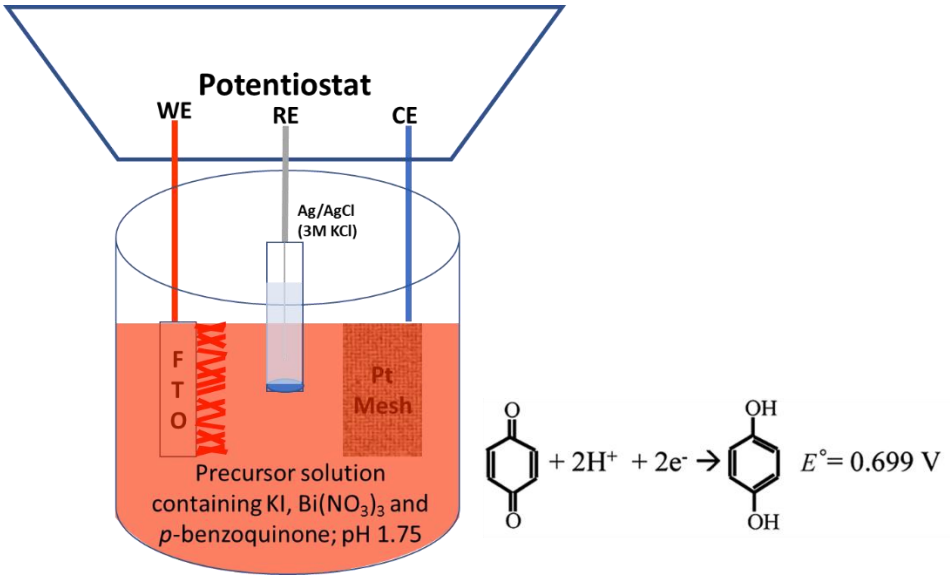

Figure S1. *Schematic illustration of the electrodeposition of BiOI nanoplates on FTO substrate*

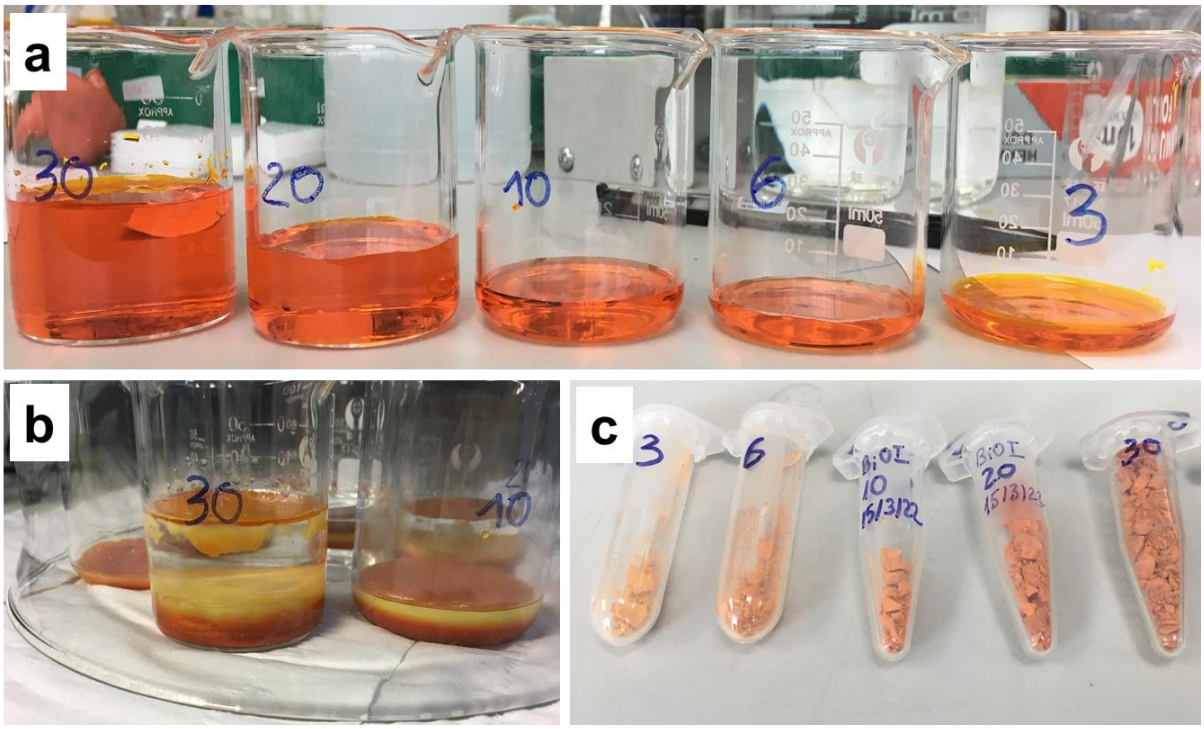

Figure S2. *Digital photos taken during the BiOI powder synthesis process. (**a**) Bi precursor solutions having different volumes (in mL); (**b**) Diffusion of NH_4OH vapor into Bi precursor solutions producing BiOI precipitates; and (**c**) The resultant BiOI powders*

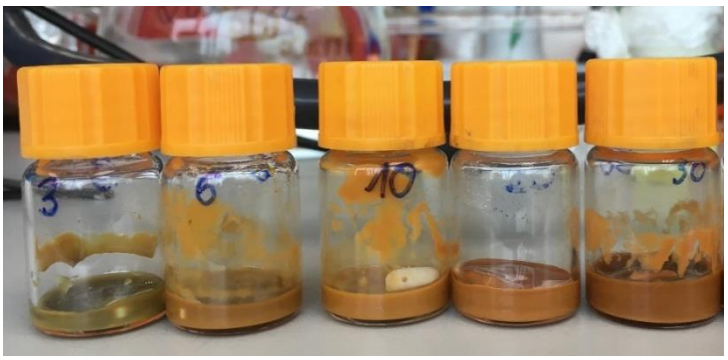

Figure S3. *Digital photos taken on the precursor inks containing BiOI nanoplates powder and VO(acac)$_2$ in dimethyl sulfoxide solvent.*

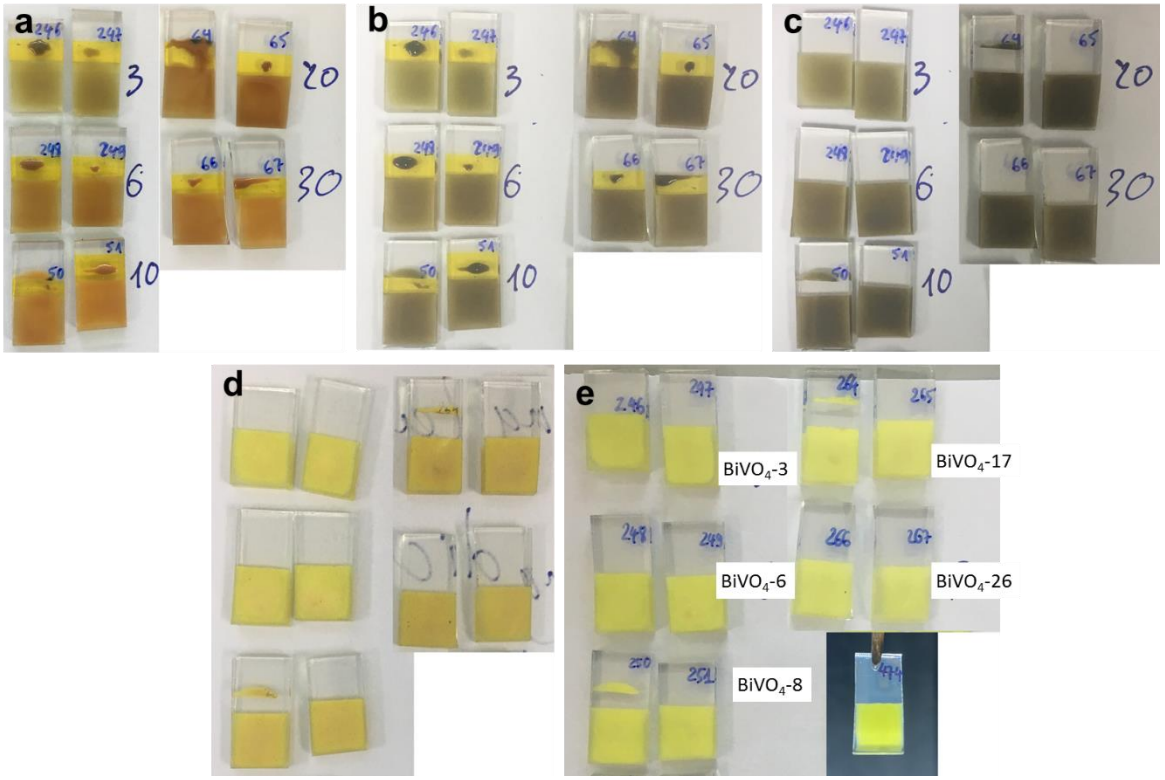

Figure S4. *Digital photos of samples during the BiVO4 films fabrication process using Doctor blade technique. (**a**) Precursor inks spread out on FTO surface; (**b**) precursor inks after being kept for 24 hours in air; (**c**) precursor inks after being dried at 70 ℃ for 1 hour; (**d**) samples after being annealed at 100 ℃ for 1 hour and then 400 ℃ for 1 hour; (**e**) the resultant BiVO$_4$ samples after removing excess V$_2$O$_5$.*

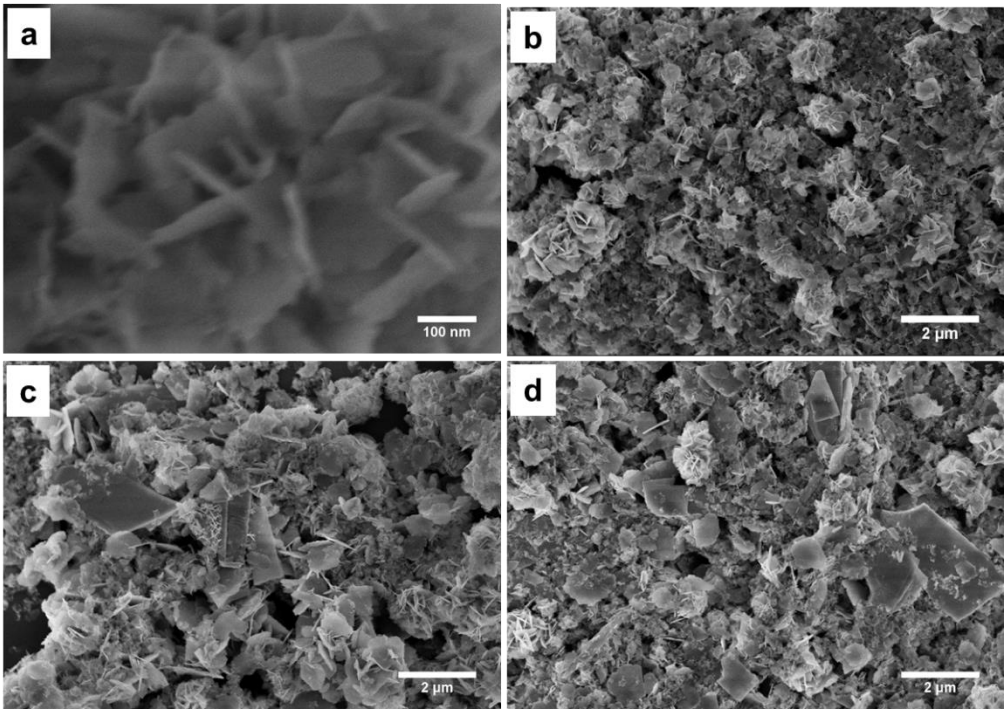

Figure S5. *SEM images taken on (**a**) BiOI-3, (**b**) BiOI-8, (**c**) BiOI-17, and (**d**) BiOI-26 samples*

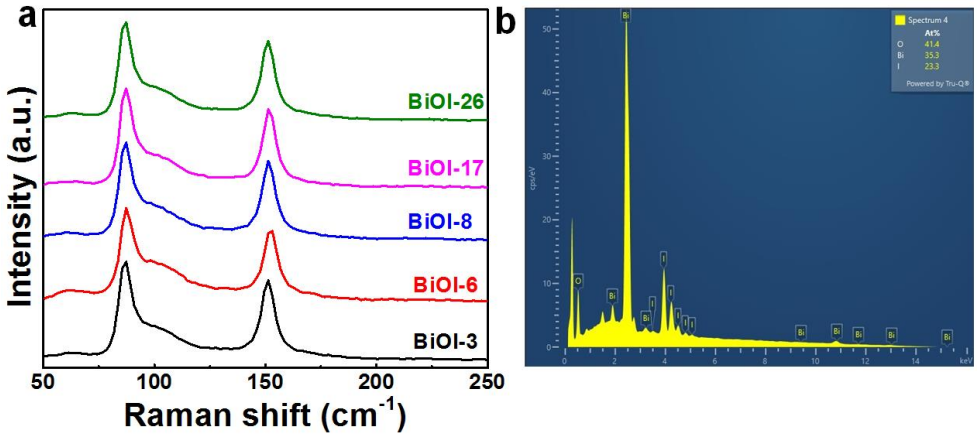

Figure S6. *(**a**) Raman spectra of BiOI samples and (b) EDX analysis of the BiOI-8 sample*

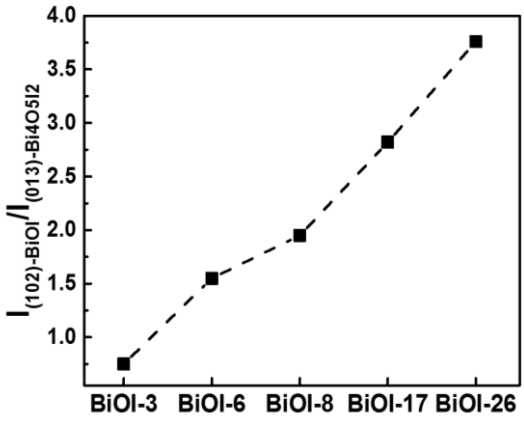

Figure S7. *Evolution of the $I_{(102)}/I_{(013)}$ peak intensity ratio in function of BiOI samples*

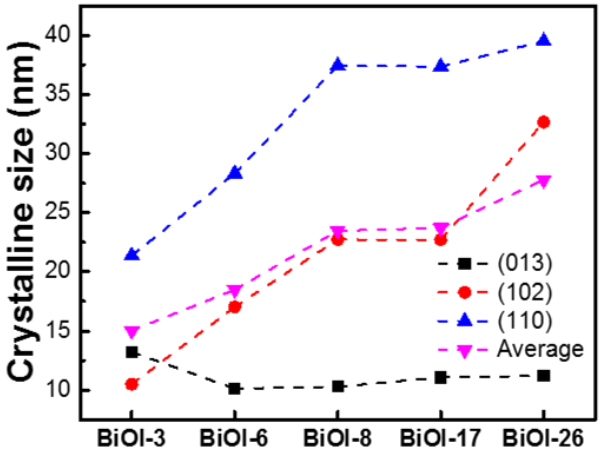

Figure S8. *Evolution of the crystalline size of BiOI samples*

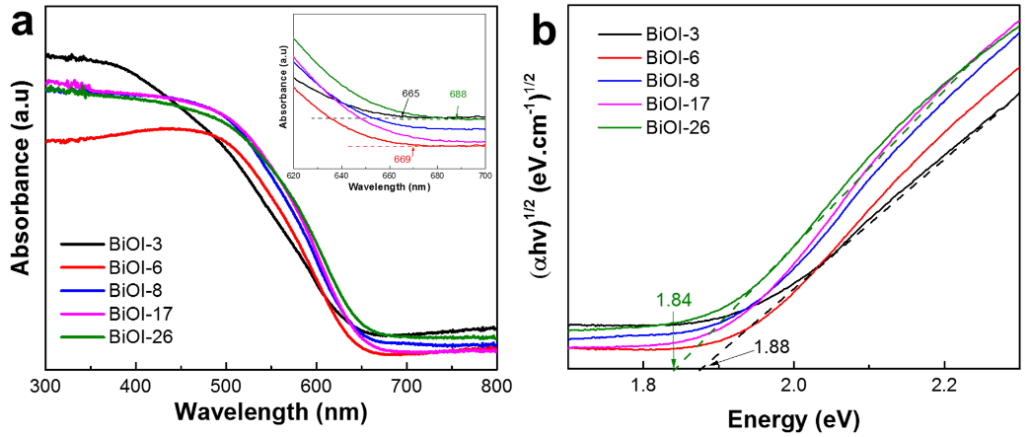

Figure S9. *(a) UV-visible diffuse reflectance spectra and (b) Tauc plot of BiOI samples*

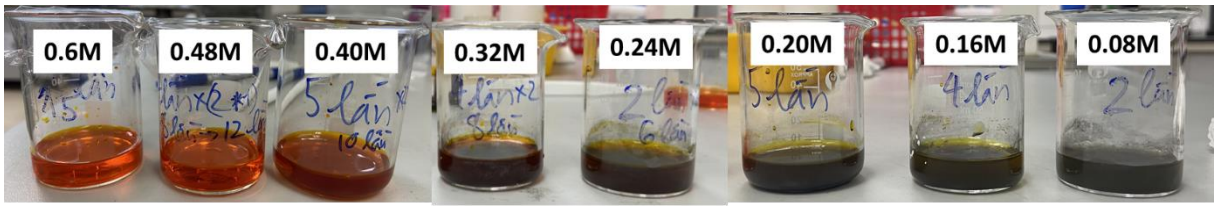

Figure S10. *Digital photos of precursor solutions constituted of 0.04M $Bi(NO_3)_3$ and different concentration of KI.*

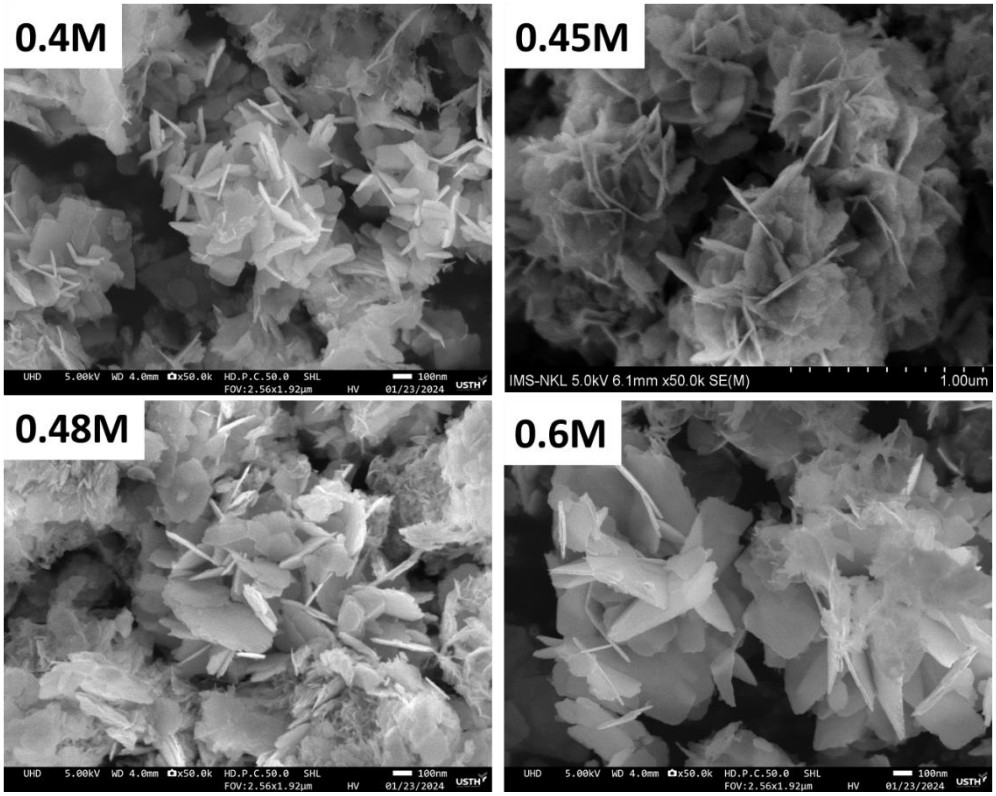

Figure S11. *SEM images of BiOI samples obtained using precursor solutions constituted of 0.04M $Bi(NO_3)_3$ and different KI concentration. KI concentration is labelled.*

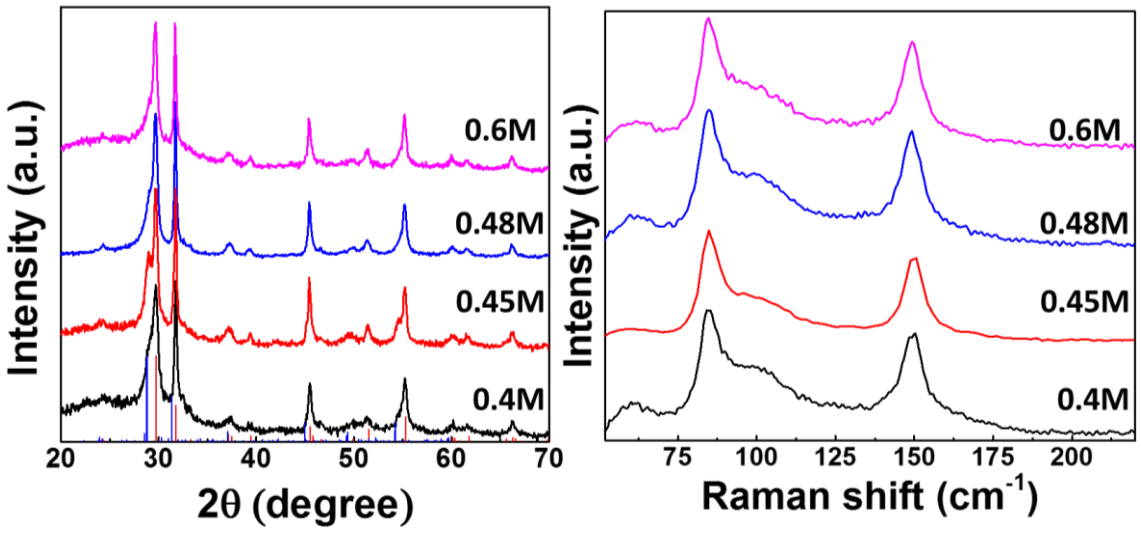

Figure S12. *XRD patterns and Raman spectra recorded for BiOI samples that were synthesized using precursor solutions constituted of 0.04M $Bi(NO_3)_3$ and different KI concentration. KI concentration is labelled.*

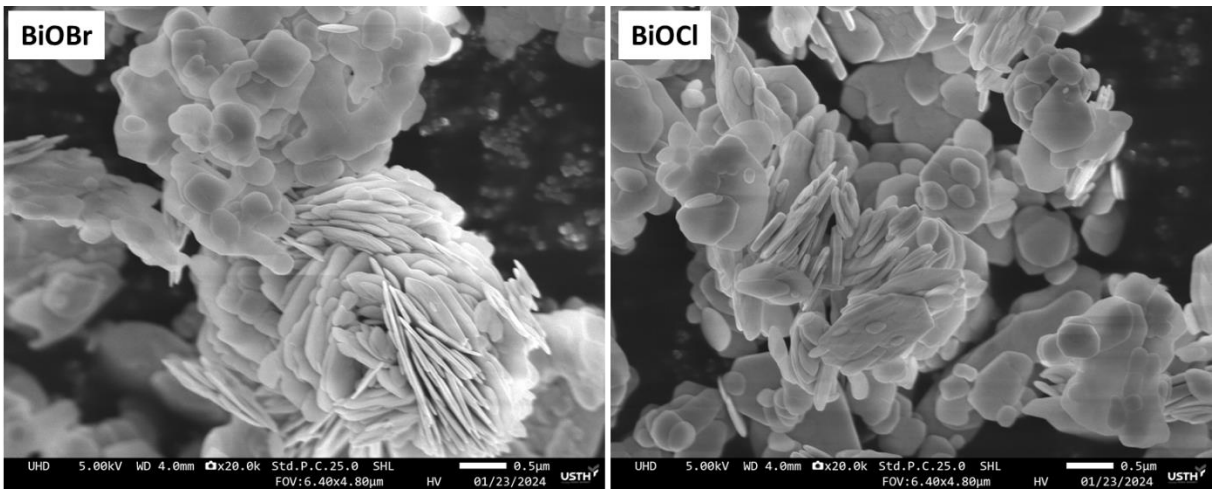

Figure S13. *SEM images of BiOCl and BiOBr powders*

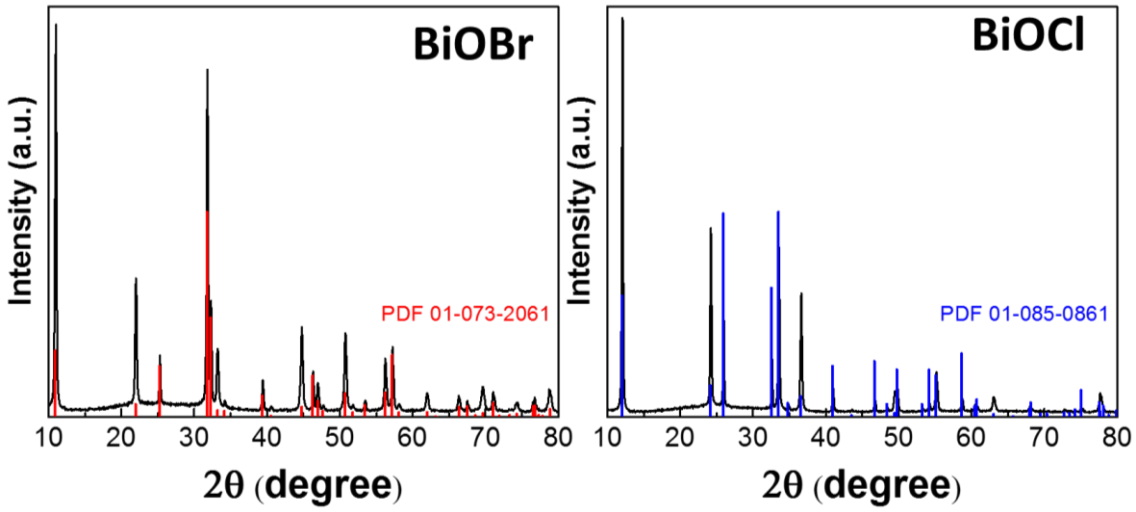

Figure S14. *XRD patterns of BiOCl and BiOBr*

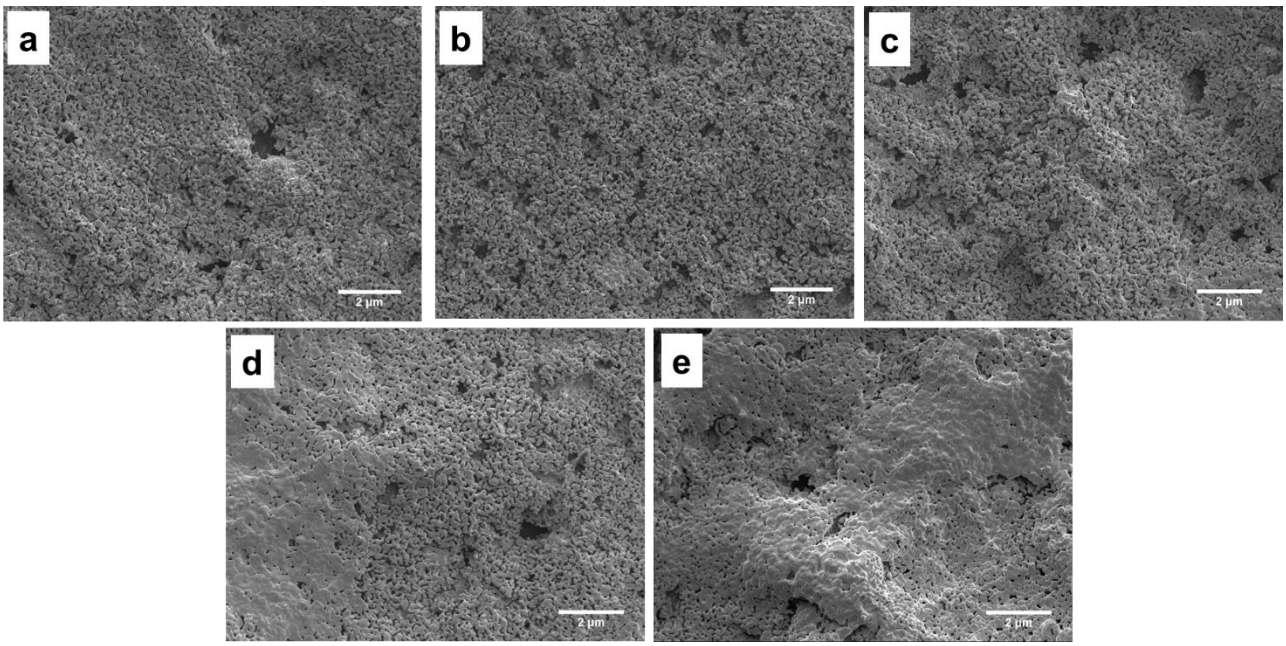

Figure S15. *SEM top-view images in low magnification of (a) $BiVO_4$-3; (b) $BiVO_4$-6; (c) $BiVO_4$-8; (d) $BiVO_4$-17 and (e) $BiVO_4$-26 films*

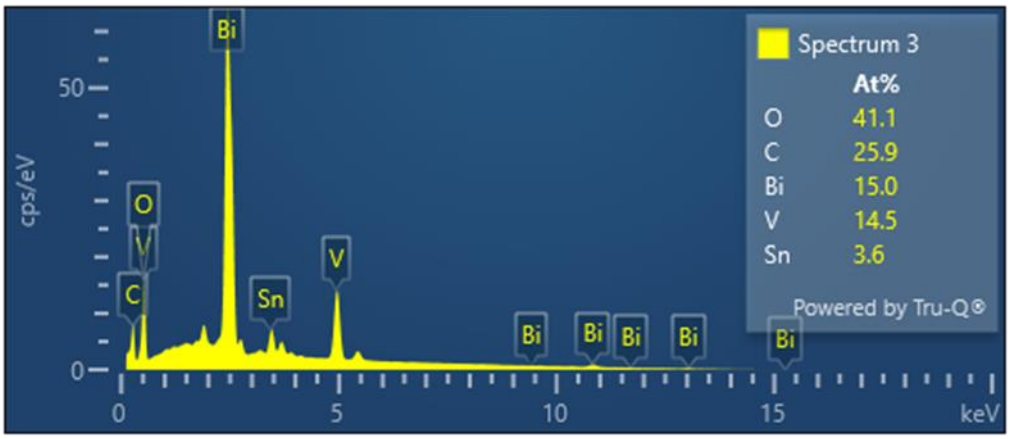

Figure S16. *EDX spectrum of $BiVO_4$-8*

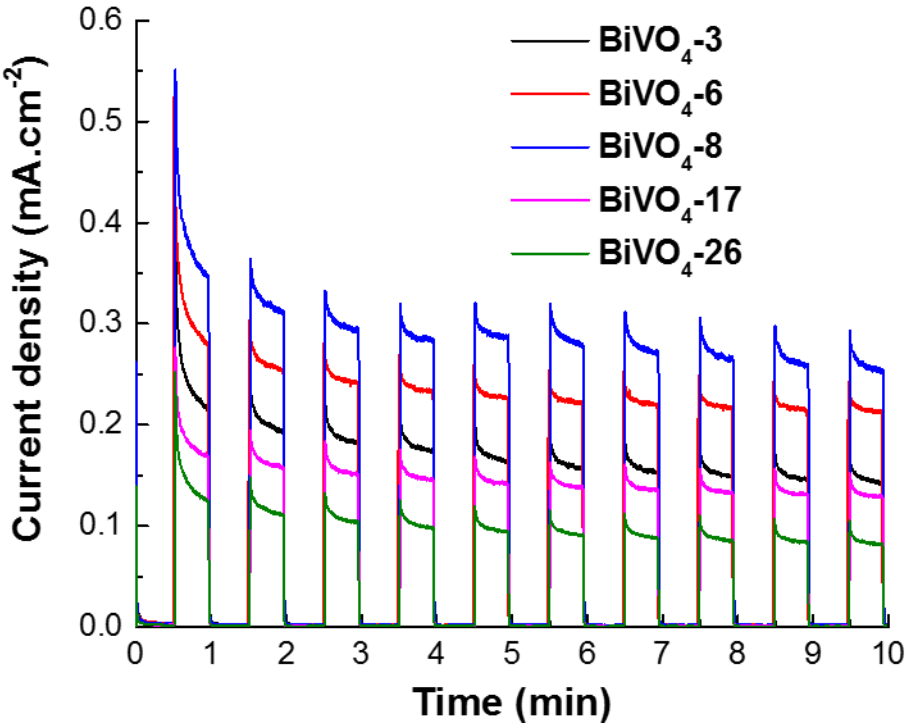

Figure S17. *I-t curves recorded for different $BiVO_4$ photoanodes held at 1.23 V_{RHE} under 1 Sun chopped-light illumination. Electrolyte was pH7 phosphate buffer solution.*

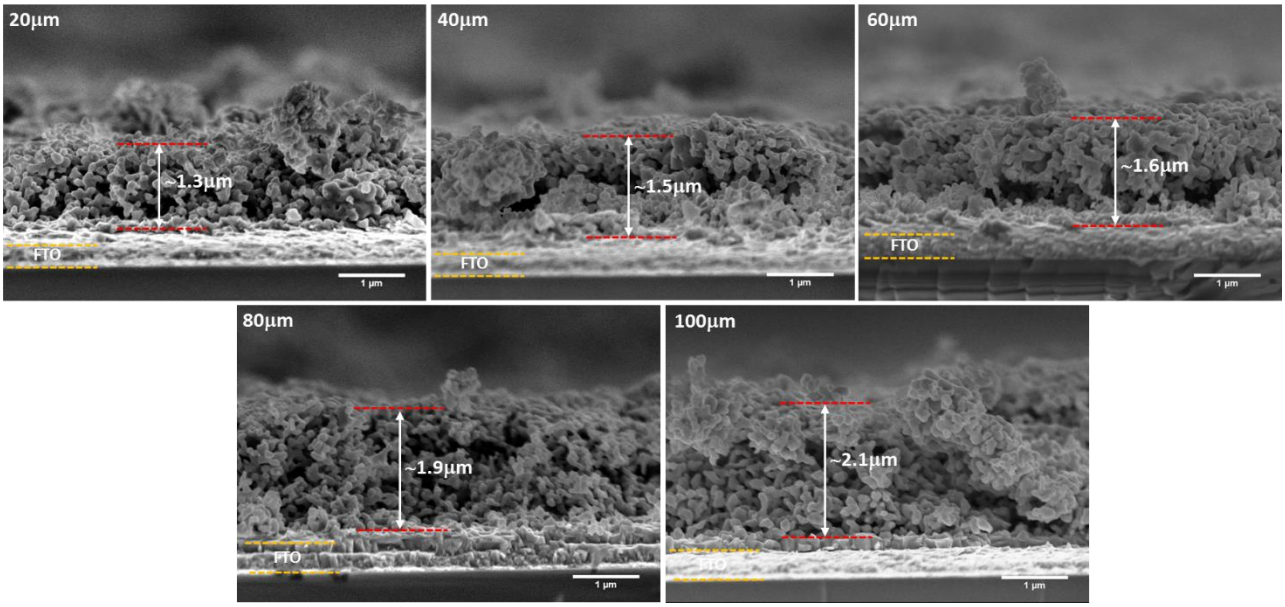

Figure S18. *SEM cross-section images of $BiVO_4$ samples obtained when varying the BiOI / $VO(acac)_2$ precursor film*

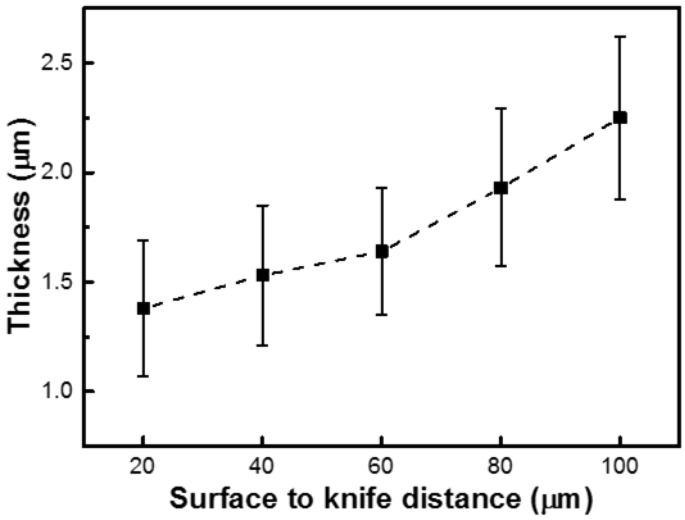

Figure S19. *Thickness of $BiVO_4$-8 thin films with different surface-to-knife distance of Doctor blade*

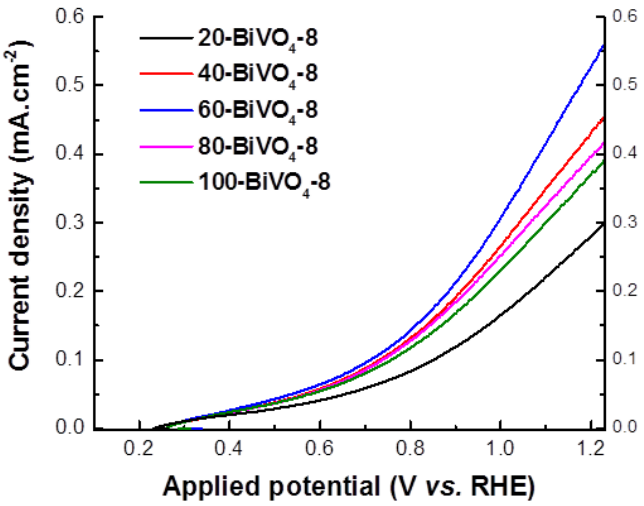

Figure S20. *LSV curves of $BiVO_4$ depended on various thickness $BiVO_4$ photoanodes*

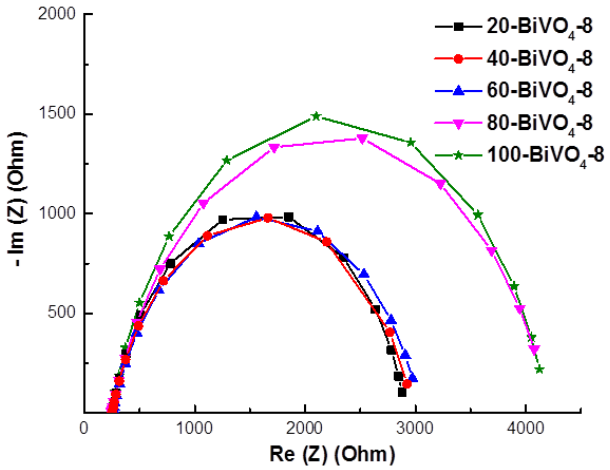

Figure S21. *Mott-Schottky of $BiVO_4$ depended on various thickness $BiVO_4$ photoanodes*

Table S1. *Crystalline size of $BiVO_4$ samples*

Sample	Crystalline size
$BiVO_4$ -3	26.8557
$BiVO_4$ -6	27.3889
$BiVO_4$ -8	27.1563
$BiVO_4$ -17	28.1042
$BiVO_4$ -26	27.0780

Table S2. *Parameters of EIS spectra fitting derived from Zview software*

Sample	Rs (Ω)	Rct (Ω)	CPE
$BiVO_4$-3	260.2	2709	0.824
$BiVO_4$-6	251.5	2717	0.795
$BiVO_4$-8	256.4	2656	0.828
$BiVO_4$-17	244	3799	0.744
$BiVO_4$-26	250.6	4243	0.822
20-$BiVO_4$-8	254	2649	0.826
40- $BiVO_4$-8	250	2730	0.793
60- $BiVO_4$-8	258	2788	0.784
80- $BiVO_4$-8	248	3787	0.791
100- $BiVO_4$-8	249	3950	0.824